Received: 1 March 2020 | Revised: 23 June 2020 | Accepted: 24 June 2020

DOI: 10.1002/nag.3125

RESEARCH ARTICLE

WILEY

A three-dimensional Hoek–Brown failure criterion based on an elliptical Lode dependence

Hua Jiang[1] | **Yang Yang**[2]

[1]School of Highway, Chang'an University, Xi'an, 710064, China

[2]Department of Civil, Environmental, and Biomedical Engineering, University of Hartford, West Hartford, CT, 06117, U.S.A.

Correspondence
Hua Jiang, School of Highway, Chang'an University, Middle Section of South Er Huan Road, Xian 710064, China.
Email: huajiang2006@hotmail.com or
Email: hkustuga@gmail.com

Funding information
Natural Science Foundation of Shaanxi Province, Grant/Award Number: 211421180224; Fundamental Research Funds for the Central Universities, Grant/Award Number: 300102218201

Summary

A new three-dimensional (3D) Hoek–Brown (HB) failure criterion based on an elliptical Lode dependence is proposed to describe failure of rocks and concrete under multiaxial stress states. This criterion not only inherits all benefits of the classical HB criterion that is developed for the triaxial compression (TXC) of rocks but also accounts for the effect of the intermediate principal stress. It is capable of representing the strength difference between the triaxial extension (TXE) and TXC with the introduction of an additional coefficient k ($0.5 \leq k \leq 1.0$), which can be derived from TXE tests or taken as 0.53 for rocks in cases where the TXE test data is unavailable. Other two material constants (m_i and σ_{ci}) involved in this criterion can be obtained from TXC tests. Additionally, the failure surface of this criterion is smooth and convex on the deviatoric stress plane when $0.5 < k$ 1.0. The new criterion achieves very good fit to the test data of TXC/TXE, biaxial compression, and polyaxial compression (PXC) on a wide variety of rock materials and concrete, reported in the literature. Comparison of the new criterion with an existing 3D HB criterion based on the same Lode dependence has demonstrated that the new criterion performs better than the latter for test data of rock and concrete under multiaxial stress states except for PXC test data of one rock type. Finally, the influence of values of k on the accuracy of the new criterion is discussed.

KEYWORDS

concrete, failure criterion, Hoek–Brown, rock, Willam–Warnke

1 | INTRODUCTION

The Hoek–Brown (HB) criterion[1–3] is one of the most widely used nonlinear failure criteria for rock mechanics and rock engineering (e.g., rock slope or borehole stability analysis). It comes with a succinct expression in terms of the major and minor principal stresses (σ_1 and σ_3, respectively) and a benefit of only requiring easily obtained material parameters. A primary feature of this criterion is that the rock failure is independent of the intermediate principal stress σ_2. However, experimental evidence has emerged to reveal the extent of σ_2 effect on the failure strength of rocks,[4–17] as summarized by Haimson[18] and Feng et al.[19] in their review papers on true triaxial compression tests of rocks. Therefore, based on experimental findings, several three-dimensional (3D) HB criteria have been proposed to account for the

effect of σ_2 and summarized by IRSM's suggested method.[20] However, none of these suggested 3D HB criteria has noncircular or convex cross sections in the deviatoric plane (see Figures 1A through 1C [21] and thus may be limited in engineering applications. To overcome this shortcoming, extensive studies have been conducted by Lee et al.,[22] Zhang et al.,[23] Jiang and Zhao,[24] and Jiang[25] et al.

For intact rocks, existing 3D HB criteria and the conventional HB criterion can be categorized as two-parameter failure criteria because only two independent material parameters m_i and σ_{ci} are involved and can be easily obtained from the triaxial compression (TXC) or polyaxial compression (PXC) test data of rocks. These 3D HB criteria can also be divided into three subcategories according to the deviatoric plane shape of their failure surfaces: one with a circular shape, the second with a noncircular and concave shape, and the third with a noncircular and convex shape that is more reasonable than the former two in terms of the plastic flow. Examples of the first subcategory include the criteria by Pan and Hudson (see Figure 1A),[26] Priest (see Figure 1B),[27] and Melkoumian et al.[28] Pan and Hudson's criterion cannot be reduced to the original HB criterion in a conventional triaxial condition ($\sigma_1 > \sigma_2 = \sigma_3$ or $\sigma_1 = \sigma_2 > \sigma_3$), which thus underestimates the TXC strength[29,30] and overestimates the biaxial strength. The latter two criteria result in a higher strength in most stress states except the TXC.[29,31] The relationship between the conventional HB criterion and this subcategory resembles that between the Mohr–Coulomb and Drucker–Prager criteria.[32] Typical examples of the second subcategory include Zhang and Zhu's 3D HB criterion (Figure 1C),[29,30] which is developed based on the Mogi criterion,[5] and Jiang's 3D HB criterion (Figure 1D)[21,33] developed from the Hsieh-Ting-Chen[34] criterion for concrete. However, these criteria may have problems with stress paths near concave points and will cause inconvenience in numerical applications.[33] The third subcategory includes criteria by Lee et al.,[22] Zhang et al.,[23] Jiang and Zhao,[24] and Jiang.[25] Among them, Lee et al.'s[22] is identical to Zhang et al.'s[23] and thus is unified with the latter and referred to as the WW 3D HB criterion in this paper, which is described in details in Section 4 with an emphasis on the advantages of the elliptical Lode dependence on the deviatoric plane over other types of Lode dependences. In summary, the second and third subcategories share the same compression and extension meridians with the conventional HB criterion and thus give a TXC strength same as the triaxial extension (TXE) strength as well as an equal biaxial compression as the uniaxial compression strengths. However, many experimental tests of rocks have already revealed that TXE strength is generally higher by 10%–20% than TXC strength.[4,35–38] Similar findings are also reported for concrete materials. For example, triaxial experiments on concrete cylinders clearly demonstrates that a substantial difference of shear strength in TXC and TXE states, which diminishes with increasing confinement[39]; equal biaxial compression strength of concrete is around 15%–16% higher than uniaxial compression strength.[40,41] Unfortunately, those 3D HB criteria with two material constants cannot reflect these characteristics of rocks or concrete.

In this research, a new 3D HB criterion is proposed for intact rocks and concrete with the use of an elliptical Lode dependence that introduces an independent coefficient k as an additional material constant, whose value can be obtained from conventional triaxial extension tests. The use of an elliptical Lode dependence facilitates a comparison between the proposed new criterion with the WW 3D HB that has been reported to have a good performance and is also formulated on the same Lode dependence, which has been widely used in practice.

The primary objective of this paper is to introduce a new use of an elliptical Lode dependence to construct a 3D HB criterion that can consider the difference in strengths of TXE and TXC. Using the same method, other new 3D HB criteria can be developed by selecting one specific Lode dependence. Thus, the proposed failure criterion can be a robust complementary to IRSM's suggested method.[20]

To evaluate applicability of the new 3D HB criterion for rocks and concrete, the TXC, TXE, biaxial compression, and PXC test data of rocks and concrete collected from published literature have been used. The application of the new criterion includes both soft and hard rocks, as the original HB criterion does. Comparisons of the new criterion with

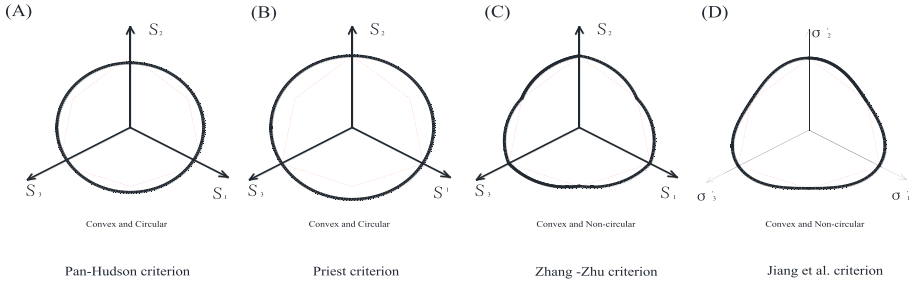

FIGURE 1 IRSM suggested method-3D HB criteria on the deviatoric plane[21] [Colour figure can be viewed at wileyonlinelibrary.com]

the WW 3D HB criterion for various stress states are also included. The influence of values of k on the accuracy of the new criterion for the PXC of rocks is discussed finally.

2 | PRELIMINARIES

A failure criterion is normally expressed in terms of principal stresses in the form of $f(\sigma_1, \sigma_2, \sigma_3)$, stress invariants in the forms of $f(I_1, J_2, \theta)$, $f(I_1, J_2, J_3)$, or $f(I_1, I_2, I_3)$, or more conveniently in the form of $f(\xi, \rho, \theta)$. The Haigh–Westergaard coordinates[42] are used to facilitate interpretation geometrically, as illustrated in Figure 2: An arbitrary point $P(\sigma_1, \sigma_2, \sigma_3)$ in the principal stress space can be described by the coordinates (ξ, ρ, θ), where ξ is the projection on the unit vector $\vec{e} = (1,1,1)/\sqrt{3}$ of the hydrostatic axis and (ρ, θ) are polar coordinates in the deviatoric plane that is orthogonal to the hydrostatic axis. The radial distance from a failure point P to the hydrostatic axis N is given by ρ, and the similarity angle θ $(0 \quad \theta \quad \pi/3)$ is measured as a rotation from the axis S_1.

$$\xi = \left|\vec{ON}\right| = I_1/\sqrt{3} = (\sigma_1 + \sigma_2 + \sigma_3)/\sqrt{3} \tag{1}$$

$$\rho = \left|\vec{NP}\right| = \sqrt{2J_2} = \frac{1}{\sqrt{3}}\sqrt{(\sigma_1 - \sigma_2)^2 + (\sigma_1 - \sigma_3)^2 + (\sigma_2 - \sigma_3)^2} \tag{2}$$

$$\theta = \frac{1}{3}\arccos\left(\frac{3\sqrt{3}}{2}\frac{J_3}{\sqrt{J_2^3}}\right) = \arccos\frac{2\sigma_1 - \sigma_2 - \sigma_3}{2\sqrt{3}\sqrt{J_2}} \tag{3}$$

$$\left|\vec{OP}\right| = \sqrt{\xi^2 + \rho^2} = \sqrt{\sigma_1^2 + \sigma_2^2 + \sigma_3^2} \tag{4}$$

where $\theta = 0$ or $\pi/3$ represents the TXC ($\sigma_1 > \sigma_2 = \sigma_3$) or TXE ($\sigma_1 = \sigma_2 > \sigma_3$) states, respectively; $0 < \theta < \pi/3$ represents the PXC condition ($\sigma_1 > \sigma_2 > \sigma_3$) that includes biaxial compression ($\sigma_3 = 0$) as a special case; and uniaxial compression ($\sigma_1 > \sigma_2 = \sigma_3 = 0$) is considered as a special case of TXC.

Principal stresses ($\sigma_1 \geq \sigma_2 \geq \sigma_3$) can be expressed in terms of ξ, ρ, and θ as[42,43]

$$\sigma_1 = \frac{\xi}{\sqrt{3}} + \sqrt{\frac{2}{3}}\rho\cos\theta \tag{5}$$

$$\sigma_2 = \frac{\xi}{\sqrt{3}} + \sqrt{\frac{2}{3}}\rho\cos\left(\frac{2\pi}{3} - \theta\right) \tag{6}$$

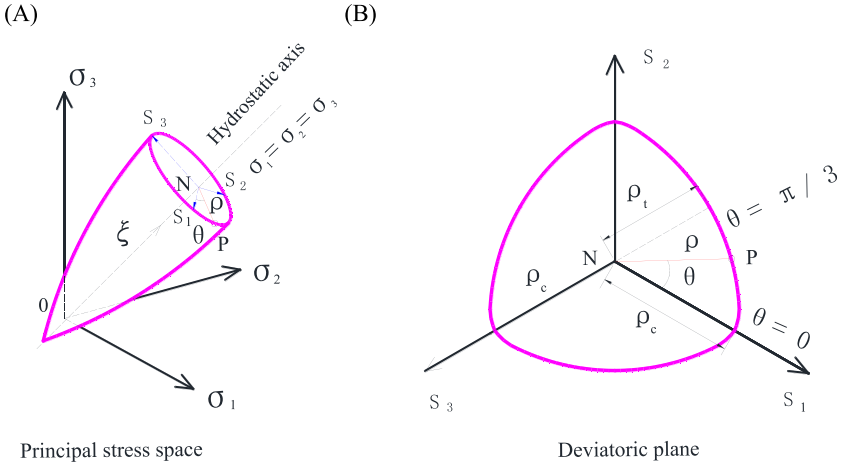

FIGURE 2 Haigh–Westergaard space and principal stress space [Colour figure can be viewed at wileyonlinelibrary.com]

$$\sigma_3 = \frac{\xi}{\sqrt{3}} + \sqrt{\frac{2}{3}}\rho\cos\left(\frac{2\pi}{3} + \theta\right) \tag{7}$$

3 | A GENERALIZED EXPRESSION OF THE HB CRITERION

The HB failure criterion is empirically developed from curve fittings of triaxial test data of rocks. A generalized form of this criterion is defined by a nonlinear relationship between the major and minor principal stresses[3]:

$$\frac{\sigma_1' - \sigma_3'}{\sigma_{ci}} = \left(m_b\frac{\sigma_3'}{\sigma_{ci}} + s\right)^a \tag{8}$$

where $\sigma_1' \geq \sigma_2' \geq \sigma_3'$ are effective principal stresses at failure with a sign convention where compression stresses are taken as positive throughout this paper; σ_{ci} is the uniaxial compression strength of an intact rock material with a petrographic constant m_i; and empirical constants m_b, s, and a can be estimated from the geological strength index (GSI) and the disturbance (D) ($0 \leq D \leq 1$) of rock masses with the following expression:

$$m_b = m_i\exp\left(\frac{GSI-100}{28-14D}\right),\ s = \exp\left(\frac{GSI-100}{9-3D}\right),\ \text{and}\ a = \frac{1}{2} + \frac{1}{6}\left[\exp\left(\frac{-GSI}{15}\right) - \exp\left(\frac{-20}{3}\right)\right] \tag{9}$$

Obviously, Equation 8 does not consider the influence of σ_2 on rock failure.

For intact rock material, GSI is taken as 100 as required,[3] and thus, values of the empirical constants in Equation 9 become

$$m_b = m_i, s = 1, \text{and}\ a = 0.5. \tag{10}$$

Substituting Equations 5 and 7 into Equation 8 gives an expression of an HB criterion formulated in terms of ξ, ρ, and θ:

$$\left[B(\theta)\frac{\rho}{\sigma_{ci}}\right]^{1/a} + m_b\left[\frac{\rho}{\sqrt{6}\sigma_{ci}}C(\theta) - \frac{\xi}{\sqrt{3}\sigma_{ci}}\right] = s \tag{11}$$

with $B(\theta) = \sqrt{2}\sin(\pi/3 + \theta)$ and $C(\theta) = 2\cos(\pi/3\text{-}\theta)$.

Figure 3 shows that $B(\theta)$ is symmetric about the axis of $\theta = \pi/6$ and ranges from $\sqrt{6}/2$ to $\sqrt{2}$, whereas $C(\theta)$ increases monotonically from 1 to 2 when 0 θ $\pi/3$.

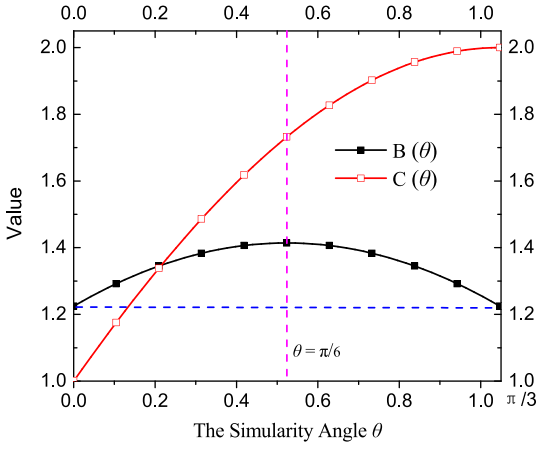

FIGURE 3 Plot of $B(\theta)$ and $C(\theta)$ as functions of θ [Colour figure can be viewed at wileyonlinelibrary.com]

When $\theta = 0$ (a TXC condition), $B(\theta=0)=\sqrt{6}/2$ and $C(\theta=0)=1$, and thus, Equation 11 becomes a compression meridian of the HB criterion

$$\left[\sqrt{1.5}\frac{\rho_c}{\sigma_{ci}}\right]^{1/a}+m_b\left(\frac{\rho_c}{\sqrt{6}\sigma_{ci}}-\frac{\xi}{\sqrt{3}\sigma_{ci}}\right)=s \tag{13}$$

When $\theta=\pi/3$ (a TXE condition), $B(\theta=0)=\sqrt{6}/2$ and $C(\theta=0)=2$, and thus, Equation 11 becomes an extension meridian of the HB criterion

$$\left[\sqrt{1.5}\frac{\rho_t}{\sigma_{ci}}\right]^{1/a}+m_b\left(\frac{2\rho_t}{\sqrt{6}\sigma_{ci}}-\frac{\xi}{\sqrt{3}\sigma_{ci}}\right)=s \tag{14}$$

For intact rocks, Equation 13 becomes a quadratic equation with respect to ρ_c/σ_{ci}, and the compressive meridian ρ_c can be expressed by

$$\rho_c=2\sqrt{6}m_i\frac{t}{\sqrt{1+36t}+1}\sigma_{ci} \tag{15}$$

$$\text{with } t=\frac{\xi}{\sqrt{3}\sigma_{ci}m_i}+\frac{1}{m_i^2} \tag{16}$$

In the same way, Equation 14 also becomes a quadratic equation with respect to ρ_t/σ_{ci} and the extension meridian ρ_t can be expressed by

$$\rho_t=\sqrt{6}m_i\frac{t}{\sqrt{1+9t}+1}\sigma_{ci} \tag{17}$$

The ratio of extension to compression medians of the HB criterion can be written as follows[25]:

$$e=\frac{\rho_t}{\rho_c}=\frac{1}{2}\frac{\sqrt{1+36t}+1}{\sqrt{1+9t}+1} \tag{18}$$

Equation 18 is used to define an elliptic function in next section, where e is a function of material constants σ_{ci} and m_i for a given ξ according to the definition of t shown in Equation 16.

4 | AN EXISTING 3D HB CRITERION BASED ON AN ELLIPTICAL LODE DEPENDENCE

Willam and Warnke[44] proposed an elliptic function to describe the failure envelope between TXC and TXE states on the deviatoric plane, which has been widely used to describe the deviatoric trace of concrete because the failure envelope is unconditionally smooth and convex for the entire range of confinements.

Lee et al.[22] and Zhang et al.[23] adopted the Willam–Warnke Lode dependence $R_3(\theta)$ to construct a 3D HB criterion, which was originally proposed by Jiang et al.[21] to construct new 3D HB criteria. This 3D HB criterion is referred to as the WW 3D HB criterion. The failure function of the WW 3D HB criterion is represented by a compressive meridian ρ_c and the ratio of extension to compression meridian radius e:

$$\rho=\rho_c R_3(\theta) \tag{19}$$

where the elliptic function $R_3(\theta)$ is defined by[21,44]:

$$R_3(\theta)=\frac{2(1-e^2)\cos(\theta-\pi/3)+(2e-1)\sqrt{4(1-e^2)\cos^2(\theta-\pi/3)+5e^2-4e}}{4(1-e^2)\cos^2(\theta-\pi/3)+(1-2e)^2} \tag{20}$$

The failure envelope surface of the WW 3D HB criterion on the deviatoric plane for different ξ is depicted in Figure 4A, where the traces are smooth and convex everywhere and circumscribe the failure envelope of the HB criterion (see dashed lines). For comparison, the new 3D HB failure criterion developed in this study is also shown with convex and smooth trace in Figure 4B, and more details about the new criterion are described in the following section.

5 | A NEW 3D HB CRITERION BASED ON AN ELLIPTICAL LODE DEPENDENCE

In this section, a new 3D HB criterion is proposed based on an elliptic Lode dependence by following procedure.

The inverse of an elliptical Lode dependence $\lambda(k, \theta)$ $[1 \le \lambda(k, \theta) \le 2]$ is described by the following equation

$$\lambda(\theta,k)=\frac{4\left(1-k^2\right)\cos^2(\theta-\pi/3)+(1-2k)^2}{2\left(1-k^2\right)\cos(\theta-\pi/3)+(2k-1)\sqrt{4\left(1-k^2\right)\cos^2(\theta-\pi/3)+5k^2-4k}} \tag{21}$$

where k is a quantity defined as the "coefficient of strength difference between TXE and TXC," which varies between 0.5 and 1.0. Influence of k on the deviatoric plane shape of the elliptical Lode dependence $1/\lambda$ (k, θ) is shown in Figure 5: The trace changes from a triangle to a circle shape with increasing k from 0.5 to 1.0. It is worth noting that

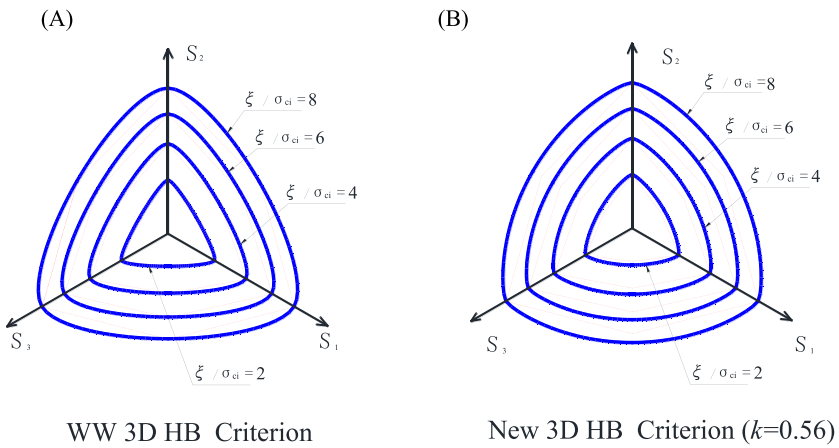

FIGURE 4 Two 3D HB failure criteria in the deviatoric plane with $m_b = 23.6$, $s = 1$, and $a = 0.5$: (A) WW 3D HB and (B) new 3D HB ($k = 0.56$) [Colour figure can be viewed at wileyonlinelibrary.com]

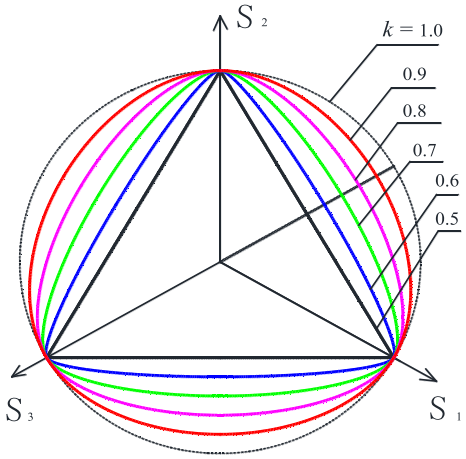

FIGURE 5 Plots of $1/\lambda$ (k, θ) at various value of k on the deviatoric plane [Colour figure can be viewed at wileyonlinelibrary.com]

the coefficient k in Equation 21 is different from e in Equation 20 because k is considered as an independent parameter in the new criterion. There are four special cases of $\lambda(k, \theta)$:

Case 1 When $\theta = 0$ (TXC), the elliptical function in Equation 21 is reduced to

$$\lambda(\theta = 0, k) = 1. \tag{22}$$

Case 2 When $\theta = \pi/3$ (TXE), the elliptical function in Equation 21 becomes

$$\lambda(\theta = \pi/3, k) = \frac{1}{k} \leq 2. \tag{23}$$

which indicates that the minimum and maximum values of $\lambda(k, \theta)$ are 1 and $1/k$, respectively.

Case 3 When $k = 0.5$ (a brittle failure), $\lambda(k, \theta)$ becomes the following special case:

$$\lambda(\theta, k = 0.5) = 2\cos(\theta - \pi/3) = C(\theta) \tag{24}$$

Herein, the Lode dependence degenerates into the transition function shown in Equation 11, which is also used in a simple 3D HB criterion.[24]

Case 4 When $k = 1$ (a ductile failure), the elliptical function $\lambda(k, \theta)$ is reduced to

$$\lambda(\theta, k = 1) = 1 \tag{25}$$

Then the Lode dependence is reduced to the Drucker–Prager circle, which is used in the Priest 3D HB criterion.[27]

Figure 6 plots the values of $\lambda(k, \theta)$ with five different values of k: the curve with $k = 0.5$ represents an upper bound and the curve with $k = 0.9$ is a lower bound. Besides, the shape of the upper bound curve is the same as $C(\theta)$ shown in Figure 3, which is consistent with Equation 24.

Through comparison between the extension and compression meridians of the HB criterion shown in Equations 13 and 14, a new 3D HB failure criterion for rocks is proposed as the following expression:

$$\left(\sqrt{1.5}\frac{\rho}{\sigma_{ci}}\right)^{1/a} + m_b\left[\frac{\rho}{\sqrt{6}\sigma_{ci}}\lambda(\theta, k) - \frac{\xi}{\sqrt{3}\sigma_{ci}}\right] = s \tag{26}$$

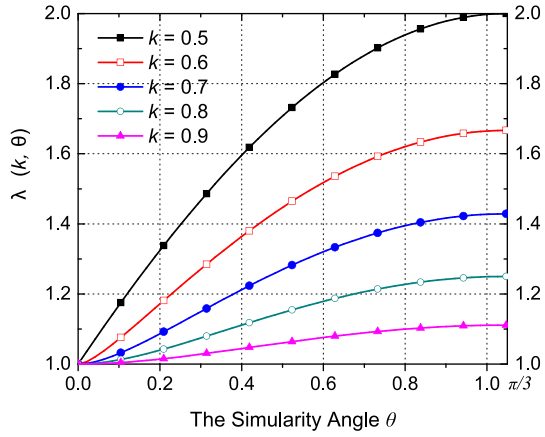

FIGURE 6 Plot of $\lambda(k, \theta)$ as functions of θ at various value of k [Colour figure can be viewed at wileyonlinelibrary.com]

where k is considered as an independent material constant to consider the strength difference between TXE and TXC and can be obtained from its extension meridian function using regression.

For intact rocks and concrete, the new 3D HB criterion by Equation 26 becomes

$$\left(\sqrt{1.5}\frac{\rho}{\sigma_{ci}}\right)^2 + m_i\left[\frac{\rho}{\sqrt{6}\sigma_{ci}}\lambda(\theta,k) - \frac{\xi}{\sqrt{3}\sigma_{ci}}\right] = 1 \tag{27}$$

Solving for ρ/σ_{ci} with Equation 27 or comparing Equation 27 with Equation 14, the new criterion can be rearranged as follows:

$$\frac{\rho}{\sigma_{ci}} = 2\sqrt{6}m_i\frac{t}{\sqrt{\lambda^2(\theta,k)+36t}+\lambda(\theta,k)} \tag{28}$$

where t is defined in Equation 16.

The extension meridian of the new criterion can be obtained by letting $\theta = \pi/3$ in Equation 28:

$$\frac{\rho_t}{\sigma_{ci}} = 2\sqrt{6}m_i\frac{t}{\sqrt{\frac{1}{k^2}+36t}+\frac{1}{k}} \tag{29}$$

Equation 29 gives a monotonic increasing function with respect to k ($0.5 \le k \le 1.0$). The extension meridian of the new criterion has a minimum value when $k = 0.5$, which reduces to the extension meridian of the HB criterion shown in Equation 17. Then the new criterion results in the same TXE strength as TXC strength. The extension meridian has a maximum value when $k = 1.0$ and becomes the compression meridian of the HB criterion shown in Equation 16. However, the predicted TXE strength is much higher than the TXC strength as reported in the Priest 3D HB criterion. Hence, in order to obtain a reasonable higher strength in TXE than in TXC, we need to set the coefficient k as $0.5 < k < 1.0$.

6 | EVALUATION OF THE NEW 3D HB CRITERION

6.1 | Test database of rocks and concrete

To evaluate the performance of the new 3D HB criterion, test data of TXC/TXE, biaxial compression, and PXC on intact rocks and concrete were collected from published literature. Table 1 summarizes the detailed information of the test data source. For example, TXC/TXE as well as PXC tests of concrete were acquired from Mills and Zimmerman's paper[39]; biaxial compression tests of rocks and concrete were conducted by Brown[7] and Kupfer et al.[40]; and PXC test data of rocks conducted by Ma and Haimson[15] and Feng et al.[16] covered a full range of the intermediate stress that varies from TXC to TXE.

6.2 | Identification of material constants

For intact rocks or concrete, there are three independent material constants (m_i, σ_{ci}, and k) involved in the new criterion as shown in Equation 27 or 28. In some cases, measured uniaxial compressive strength σ_{ci} is provided, and then only two material constants m_i and k need to be determined from test data. These material constants are identified from conventional triaxial tests because this type of data is usually available in practice.[45] For example, constants m_i and σ_{ci} can be obtained through regression on TXC data according to its compression meridian function in terms of ξ, ρ, and θ as shown in Equation 16 or in terms of the principal stresses:

$$\frac{\sigma_1'}{\sigma_{ci}} = \frac{\sigma_3'}{\sigma_{ci}} + \sqrt{m_i\frac{\sigma_3'}{\sigma_{ci}}+1} \tag{30}$$

TABLE 1 Test data source of rock and concrete

No.	Type	Investigator(s)	Stress state	Specimen size
1	Dunham dolomite	Mogi (1967[4], 2007)[6]	TXC, TXE	Circular cylinders 1.6 cm × 5.0 cm
2	Westerly granite	Mogi (1967[4], 2007)[6]	TXC, TXE	Circular cylinders 1.6 cm × 5.0 cm
3	Phra Wihan sandstone	Phueakphum et al. (2013)[37]	TXC, TXE	Cubic 5.5 cm × 5.5 cm × 5.5 cm
4	Phu Kradung siltstone	Phueakphum et al. (2013)[37]	TXC, TXE	Cubic 5.5 cm × 5.5 cm × 5.5 cm
5	Saraburi marble	Phueakphum et al. (2013)[37]	TXC, TXE	Cubic 5.5 cm × 5.5 cm × 5.5 cm
6	Concrete	Mills and Zimmerman (1970)[39]	TXC, TXE	Circular cylinders 7.62 cm × 15.24 cm
7	Wombeyan marble	Brown (1974)[7]	Biaxial compression	Rectangular prism 7.6 cm × 7.6 cm × 2.5 cm
8	Concrete	Kupfer et al. (1969)[40]	Biaxial compression	Rectangular prism 20 cm × 20 cm × 5 cm
9	Sandstone	Feng et al. (2019)[16]	PXC	Rectangular prism 5 cm × 5 cm × 10 cm
10	Coconino sandstone	Ma and Haimson (2006)[14]	PXC	Rectangular prism 1.9 cm × 1.9 cm × 3.8 cm
11	Mizuho trachyte	Mogi (1971[5], 2007)[6]	PXC	Rectangular prism 1.5 cm × 1.5 cm × 3.0 cm
12	Shirahama sandstone	Takahashi and Koide (1989)[10]	PXC	Rectangular prism 3.5 cm × 3.5 cm × 7.0 cm
13	Yuubari shale	Takahashi and Koide (1989)[10]	PXC	Rectangular prism 3.5 cm × 3.5 cm × 7.0 cm
14	Concrete	Mills and Zimmerman (1970)[39]	PXC	Circular cylinders 7.62 cm × 15.24 cm

Abbreviations: PXC, polyaxial compression; TXC, triaxial compression; TXE, triaxial extension.

Equation 30 is obtained by substituting Equation 10 into Equation 8. The compression meridian of the new criterion is the same as that of the HB criterion (or the WW 3D HB criterion).

With available values of m_i and σ_{ci}, the constant k can be obtained through regression on TXE data according to the extension meridian of the new criterion formulated in terms of ξ, ρ, and θ as shown in Equation 29 or in terms of the principal stresses expression as

$$\frac{\sigma_1'}{\sigma_{ci}} = \frac{1}{6}\left[6\frac{\sigma_3'}{\sigma_{ci}} + \left(2-\frac{1}{k}\right)m_i + \sqrt{\left(\frac{1}{k}-2\right)^2 m_i^2 + 36\left(1+m_i\frac{\sigma_3'}{\sigma_{ci}}\right)}\right] \tag{31}$$

Equation 31 can be derived from Equation 29, and when $k = 0.5$, it is reduced to Equation 30, which implies that the new criterion's extension meridian becomes the HB criterion's and is the same as the HB criterion's compression meridian because the influence of σ_2 is neglected. For a given value of σ_3', the failure strength in TXE and TXC states can be easily obtained from Equation 31 by inputting estimated k (>0.5) and $k = 0.5$, respectively. In the absence of TXE data, $k = 0.53$ is empirically suggested for PXC of rocks in this research.

In biaxial compression states ($\sigma_3 = 0$), the failure strength is always greater than the uniaxial compression strength ($\sigma_2 = \sigma_3 = 0$) because of the effect of σ_2.[7,40] The biaxial compression strength at a given value of σ_2 can be estimated from the uniaxial compression strength σ_{ci}, the uniaxial tension strength f_t, and the equibiaxial compression strength f_{cc}. In biaxial states, the new criterion for intact rocks and concrete in Equation 27 can be expressed in terms of principal stresses by substituting Equations 1 and 2 into Equation 27

$$\frac{\sigma_1'^2+\sigma_2'^2-\sigma_1'\sigma_2'}{\sigma_{ci}^2} + \frac{1}{3}\lambda(\theta,k)m_i\frac{\sqrt{\sigma_1'^2+\sigma_2'^2-\sigma_1'\sigma_2'}}{\sigma_{ci}} - m_i\frac{\sigma_1'+\sigma_2'}{3\sigma_{ci}} = 1 \tag{32}$$

In an equibiaxial compression state ($\sigma_1 = \sigma_2 = f_{cc}$ and $\sigma_3 = 0$), the stress state with $\theta = \pi/3$ lies in the extension meridian of the new criterion. Substituting the stress state (f_{cc}, f_{cc}, 0) and $\lambda(\theta, k) = 1/k$ into Equation 32, a simplified expression can be obtained as follows:

$$\frac{f_{cc}^2}{\sigma_{ci}^2} + m_i\frac{f_{cc}}{\sigma_{ci}}\frac{1-2k}{3k} = 1 \tag{33}$$

In a uniaxial tension ($\sigma_1 = \sigma_2 = 0$, $\sigma_3 = -f_t$), the new criterion can be expressed in a similar form as Equation 33:

$$\frac{f_t^2}{\sigma_{ci}^2} + m_i \frac{f_t}{\sigma_{ci}} \frac{1+k}{3k} = 1 \tag{34}$$

Combining Equation 33 and Equation 34, material constant k of the new criterion can be expressed in terms of f_{cc} and f_t:

$$\frac{1-2k}{1+k} = \frac{1/(f_{cc}/\sigma_{ci}) - f_{cc}/\sigma_{ci}}{1/(f_t/\sigma_{ci}) - f_t/\sigma_{ci}} \tag{35}$$

When f_{cc}/σ_{ci} and f_t/σ_{ci} are provided in test data, k can be estimated according to Equation 35, and thus, the material constant m_i can be further obtained from Equation 33 or Equation 34 by substituting k into one of them.

6.3 | Comparison of the new criterion with experimental data

6.3.1 | Conventional TXC and TXE

Figure 7 shows conventional TXC and TXE tests for five different rock types and concrete, in which σ_1 and σ_3 are normalized with respect to the uniaxial compression strength σ_{ci} of rocks. It is clearly shown that the TXE strength is higher than the TXC one. The dashed curves represent the best-fitting curve according to Equation 30 predicted by the WW 3D HB criterion, which shows the same TXE and TXC strength values. The two separate solid curves refer to the best-fitting curves using the new criterion with $0.5 < k < 1.0$, in which value of m_i is obtained through regression on TXC data according to Equation 30 and values of k is obtained on TXE data according to Equation 31. If the intermediate principal stress σ_2 was not an influence factor, the curve of σ_1 versus σ_3 for extension tests would coincide with the curve for compression. It is obvious that the two solid curves fit the test data much better than the single dashed curve as indicted by the coefficient of determination (DC) in each figure. The DC of the dashed curves ranges from −0.03 to 0.919, whereas the DC of the solid curves ranges from 0.912 to 0.979 for TXE and from 0.950 to 0.999 for TXC. The best-fit value of k obtained using the new 3D HB criterion for five rock types ranges from 0.528 to 0.551. Hence, $k = 0.53$ is used for rocks in Section 6.3.3 when there is no TXE data available for rocks. For concrete, the best-fitted value of k obtained using the new 3D HB criterion is 0.56 with a DC of 0.967 for TXE states, and a DC of 0.987 for TXC states. In comparison, the value of DC corresponding to the single dashed curve is 0.919. It is worth noting that σ_{ci} is considered as an unknown material constant for concrete because five different values of σ_{ci} ranging from 21.2 to 26.8 MPa exist in the test data. Table 2 summarizes the best-fit values of σ_{ci}, m_i, k, and DC for TXC and TXE states obtained with the new criterion. Table 3 summarizes the best-fit values of m_i, σ_{ci}, and DC obtained with the WW 3D HB criterion.

6.3.2 | Biaxial compression

Figure 8A compares a set of biaxial compression test data of Wombeyan marbles by Brown[7] with the predicted failure envelope in a biaxial plane ($\sigma_3 = 0$) using the new and the WW HB criteria, in which five different stress ratios ($\sigma_2/\sigma_1 = 0.0$, 0.25, 0.50, 0.75, and 1.0) are reported and the biaxial compression strength is obviously higher than the uniaxial compression strength. The experimental equibiaxial compression strength f_{cc} is 1.03 σ_{ci}, and the uniaxial tension strength of marble f_t is assumed to be 0.08 σ_{ci}.[46] The calculated values of material constants according to Equations 34 and 35 are $m_i = 12.48$ and $k = 0.503$, respectively. A good fit to the test data using the new criterion is illustrated by the solid line. In contrast, the predicted curve using the WW 3D HB criterion with $m_i = 12.42$ (see the dashed line) does not work well for biaxial compression of rocks.

In Figure 8B, the predicted biaxial compression curves of two 3D HB criteria are compared with the test data by Kupfer et al.,[40] where $f_{cc} = 1.16\ \sigma_{ci}$ and $f_t = 0.09\ \sigma_{ci}$ are reported. The estimated values of material constants according to Equations 34 and 35 are $m_i = 11.32$ and $k = 0.521$, respectively. The results obtained using the new criterion

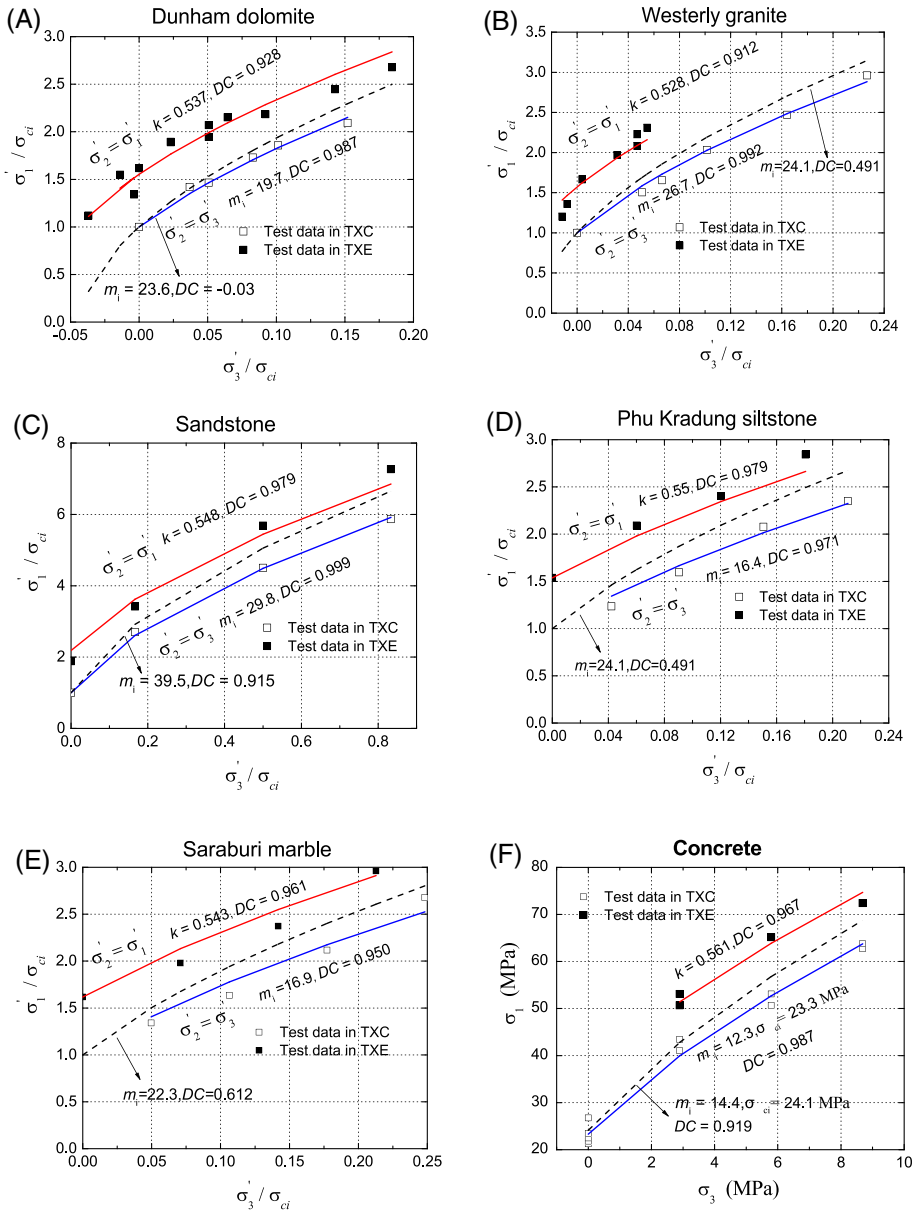

FIGURE 7 Comparisons of experimental data with the best-fit curves using the new 3D HB (solid lines) and WW 3D HB (dashed lines) criteria for rocks and concrete in TXC/TXE [Colour figure can be viewed at wileyonlinelibrary.com]

TABLE 2 Calibration of the new 3D HB criterion against TXC and TXE data of rocks and concrete

No.	Test data	σ_{ci} (MPa)	m_i	k	DC (TXC/TXE)
a	Dunham dolomite	217 (test data)	19.7	0.537	0.987/0.928
b	Westerly granite	256 (test data)	26.7	0.528	0.992/0.912
c	Sandstone	60 (test data)	29.8	0.548	0.999/0.979
d	Phu Kradung siltstone	NA	16.4	0.551	0.971/0.977
e	Saraburi marble	NA	16.8	0.543	0.950/0.961
f	Concrete	23.3	12.3	0.561	0.987/0.967

Abbreviation: NA, not applicable.

are much better than those obtained using the WW 3D HB criterion with $m_i = 22.04$. The reason may be that the tested value of f_{cc} is much larger than the tested σ_{ci} for concrete, which, however, cannot be described by the WW 3D HB criterion.

TABLE 3 Calibration of the WW 3D HB criterion against TXC and TXE data of rocks and concrete

No.	Test data	σ_{ci} (MPa)	m_i	*DC*
a	Dunham dolomite	217 (test data)	23.6	−0.03
b	Westerly granite	256 (test data)	24.1	0.491
c	Sandstone	60 (test data)	39.5	0.915
d	Phu Kradung siltstone	NA	24.1	0.491
e	Saraburi marble	NA	22.3	0.612
f	Concrete	24.1	14.4	0.919

Abbreviation: NA, not applicable.

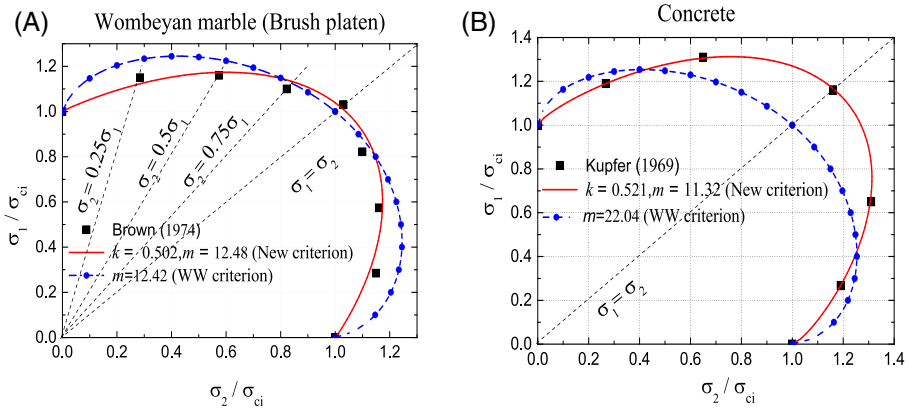

FIGURE 8 Comparisons of two 3D HB criteria with biaxial compression tests of: (A) Wombeyan marble and (B) concrete [Colour figure can be viewed at wileyonlinelibrary.com]

6.3.3 | PXC tests

Figures 9A, through 9E compares the predicted curves with PXC test data in the $\sigma_1'-\sigma_2'$ plane for five different rock types with values of uniaxial compression strength σ_{ci} available for two types. PXC, TXC, TXE, and those data with the same value of σ_3' are joined and marked with a common symbol. The solid lines represent the theoretical $\sigma_1'-\sigma_2'$ relationship predicted by the new criterion. For a given σ_3', when the intermediate principal stress σ_2' increases from $\sigma_2'=\sigma_3'$ (corresponding to a TXC state) to $\sigma_2'=\sigma_1'$ (corresponding to a TXE state), the predicted strength σ_1' initially increases, then reaches the maximum value at a specific value of σ_2', and eventually decreases to a value that is larger than the TXC strength at the same value of σ_3'. The dashed curves represent the best-fitting results predicted by the WW 3D HB criterion. Different from the solid lines, the predicted failure strength finally decreases to a value, which is same as the TXC strength. Additionally, the solid curves insect with the dashed at specific values of σ_2' (denoted as $\sigma_{2,\text{intersect}}'$). Values of material constants m_i and σ_{ci} used for plotting the theoretical curves are summarized in Table 4, which are obtained through regression on TXC test data. The new and the WW 3D HB criteria have the same compressive meridian as the HB criterion and thus result in same values for the material constants σ_{ci} and m_i.

The value of the material constant k involved in the new criterion is empirically assumed to be 0.53 if there is no TXE test data available for rocks. For sandstone in Figure 9A, $k = 0.548$ is obtained from TXE test data, which is also shown in Figure 7C. The new criterion fits the test data much better than the WW 3D HB criterion because TXE strength is about 23.8%–88.3% higher than TXC strength for the same σ_3 in the test data, which cannot be captured by the WW 3D HB criterion. For Coconino sandstones, $k = 0.51$ is obtained from TXE test data with $\sigma_{ci} = 77.7$ MPa and $m_i = 17.6$ determined from TXC tests. It is worth noting that the failure strength predicted by the WW 3D HB criterion is higher than that by the new criterion when the intermediate principal stress σ_2' increases from σ_3' to $\sigma_{2,\text{intersect}}'$, whereas, on the contrary, the former is lower than the latter when σ_2' ranges from $\sigma_{2,\text{intersect}}'$ to σ_1'.

Figure 9F shows the predicted failure envelope in the $\sigma_1'-\sigma_2'$ plane for concrete, in which $\sigma_2$varies from TXC to TXE states. The best-fitting set of material constants ($k = 0.561$, $m_i = 12.3$, and $\sigma_{ci} = 23.3$ s MPa) is from TXC and TXE tests (see Figure 7D). It can be observed that the new criterion fits the test data better than the WW 3D HB criterion in each confining pressure. The reason is that the material constant k in the new criterion is directly obtained through regression on the TXE test data, whereas the fact that the TXE strength is higher than the TXC strength cannot be captured by the WW 3D HB criterion.

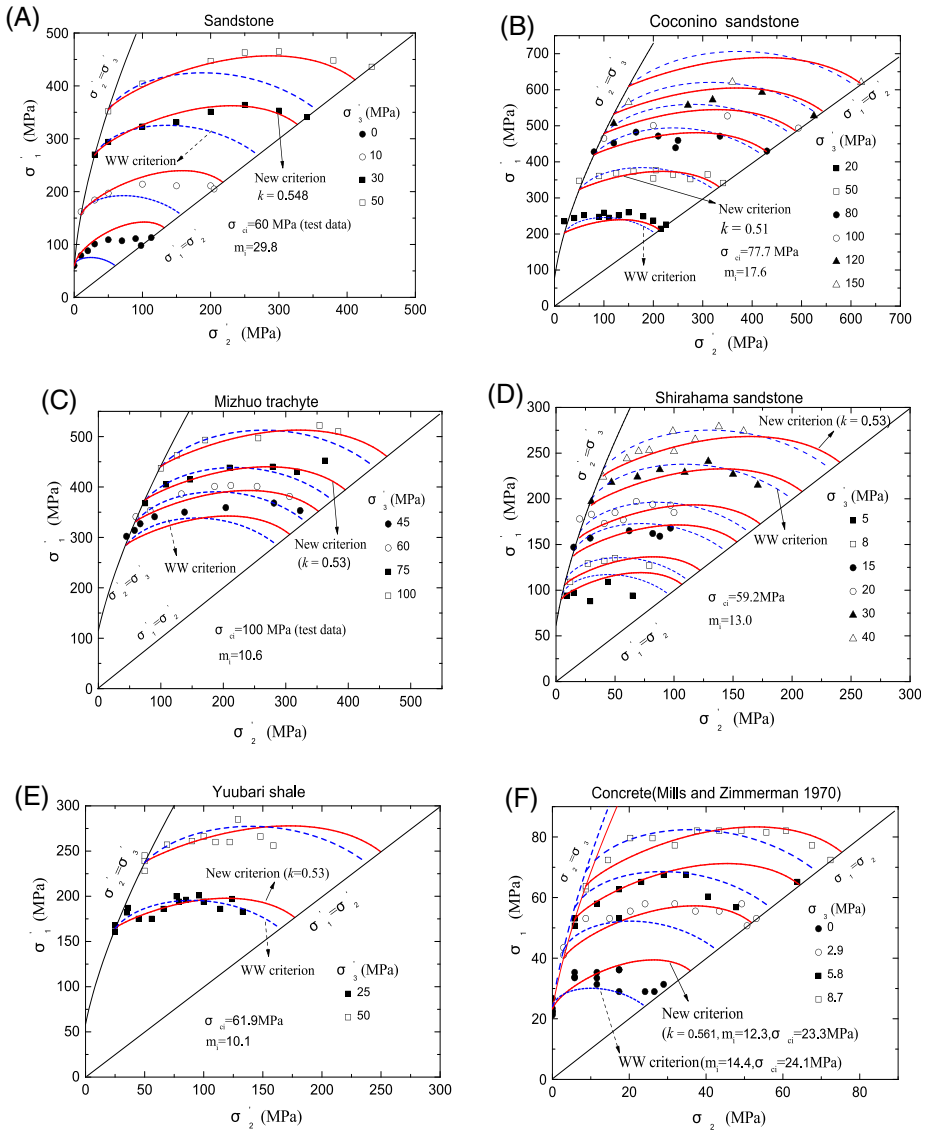

FIGURE 9 Comparisons of the new 3D HB and WW 3D HB criteria with PXC data for rocks and concrete in the $\sigma_1' - \sigma_2'$ plane [Colour figure can be viewed at wileyonlinelibrary.com]

TABLE 4 Best-fitting material constants and *DC* for PXC of rocks and concrete using the new 3D HB criterion

No.	Test data	m_i (range)	m_i	σ_{ci} (MPa)	k	*DC* (TXC/TXE)
a	Sandstone	13–21	29.8	60.0	0.548	0.999/0.979
b	Coconino sandstone	13–21	17.6	77.7	0.51	0.981/0.996
c	Mizuho trachyte	9–17	10.61	(100)	0.53	0.979/NA
d	Shirahama sandstone	13–21	13.0	59.2	0.53	0.768/NA
e	Yuubari shale	4–8	10.1	61.9	0.53	0.974/NA
f	Concrete	-	12.3	23.3	0.561	0.987/0.967

Note: () means that σ_{ci} is provided in the tests; $k = 0.53$ is empirically set for five rock types due to lack of TXE data; NA, not applicable.

Figure 10 further compares the root-mean-square error (RMSE)[24,25] resulted from two 3D HB criteria for the PXC strength of rocks and concrete. The RMSE is defined in terms of the major principal stress as $\mathrm{RMSE} = \sqrt{\sum_{i=1}^{n} \left(\sigma_{1i}^{\mathrm{calc}} - \sigma_{1i}^{\mathrm{test}}\right)^2 / n}$, where n is the number of test data for each rock type or concrete and $\sigma_{1i}^{\mathrm{calc}}$ and $\sigma_{1i}^{\mathrm{test}}$ represent the ith calculated and tested values of the failure strength, respectively. In comparison, the new criterion

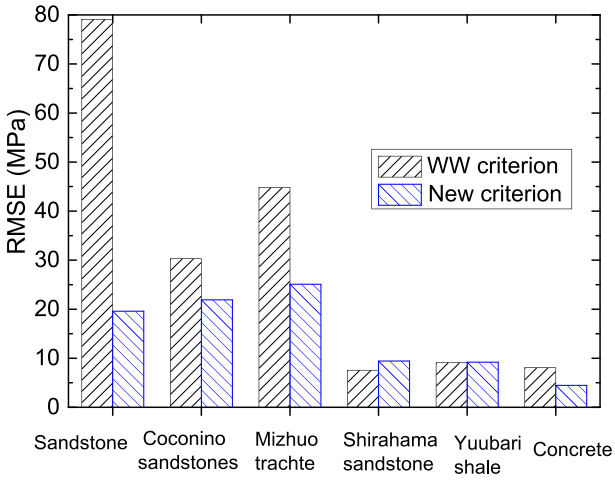

FIGURE 10 Comparisons of RMSE of σ_1 obtained using two 3D HB criteria for rocks and concrete in PXC [Colour figure can be viewed at wileyonlinelibrary.com]

performs better than the WW 3D HB criterion for three rock types (Sandstone, Coconino sandstone, and Mizhuo trachyte) and concrete, whereas the latter performs slightly better than the former for Shirahama sandstones.

Based on the discussions above, it can be concluded that the new criterion performs better than the WW 3D HB criterion in most rock types and concrete.

6.3.4 | Influence of k

In Section 6.3.3, k is assumed as 0.53 in the new criterion for all rock types when TXE data are unavailable; however, the assumed value may not be the best-fit for k. Taking Mizhuo trachytes for an example (see Figure 9C), the new criterion with $k = 0.53$ tends to underestimate the rock strength near a TXE state especially with a low confining pressure ($\sigma_3' = 45$ or 60 MPa). Therefore, the influence of k (ranging from 0.50 to 0.58) on the RMSE of σ_1' for this type of rock is further discussed as follows.

In Figure 11A, the RMSE decreases from 78.2 to 15.0 MPa when k increases from 0.50 to 0.56 and then increases again to 19.9 MPa when k is larger than 0.56. Hence, the best-fit value of k for Mizhuo trachytes is 0.56 with the minimum value of the RMSE (15.0 MPa), which is much smaller than the value (25.1 MPa) when $k = 0.53$ as shown in Figure 9C.

Figure 11B plots the curve of the new criterion in the $\sigma_1' - \sigma_2'$ plane for Mizhuo trachytes with the best-fit $k = 0.56$. A good agreement with test data in low confining pressures ($\sigma_3' = 45$ or 60 MPa) can be observed. It is worth noting that the best-fit value of k may depend on the rock type, and a better estimation on the value can be achieved on the TXE data.

Finally, it is worthy to be noted that the proposed failure criterion is for intact rocks and may be extended to cross-anisotropic rocks by using a second-order fabric tensor to describe anisotropic structure of the material.[47,48] However, there is few polyaxial compression test data of anisotropic rock available to validate such criteria.[22,49,50] Hence, application of proposed failure criterion is focused on isotropic intact rocks with a wide variety of test data in this paper.

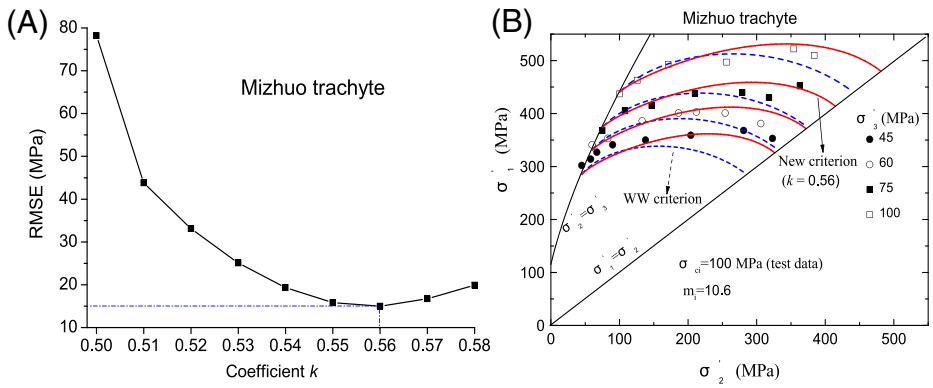

FIGURE 11 Comparisons of the new criterion with PXC test data of Mizhuo trachyte: (A) the influence of k on RMSE and (B) the prediction results corresponding to the best-fit value of k in the $\sigma_1' - \sigma_2'$ plane [Colour figure can be viewed at wileyonlinelibrary.com]

7 | CONCLUSIONS

A new 3D HB failure criterion based on an elliptical Lode dependence is proposed to describe failure of rocks and concrete under complex stress states, in which the effect of σ_2 is considered. The new criterion inherits the compression meridian of the HB criterion and introduces an additional coefficient $k(0.5 \leq k \leq 1)$ to define its extension meridian. The involved material constants σ_{ci} and m_i can be estimated from the TXC test data (same as the HB criterion), and the third material constant k can be identified from TXE tests. In the absence of the TXE data, an empirical value of 0.53 is suggested for k.

When $k = 0.5$, the extension meridian of the new criterion is reduced to that of the HB criterion. The proposed new criterion reduces to a simple 3D HB criterion[24] proposed by the first author. When $k = 1$, the compression meridian of the new criterion becomes that of the HB criterion. The new criterion becomes the 3D HB criterion by Priest.[27] When $0.5 < k \leq 1$, the fact that the TXE strength is higher than the TXE strength can be captured by the new criterion and the magnitude of the difference between the TXC and TXE strengths is a function of the value of k.

The TXC/TXE, biaxial compression, and PXC test data of rocks and concrete are collected from literature and used to evaluate the performance of the new criterion. The evaluation results reveals a good fit to the test data using the new criterion for all different stress states. Comparison between the new criterion and the WW 3D HB demonstrates that the new criterion performs better than the latter for the PXC data of three rock types and concrete except for one rock type. The assumed value of k was found to have a significant influence on the accuracy of the new criterion when TXE data of rocks is unavailable. Besides, the new criterion performs much better than the WW 3D HB criterion for the biaxial compression of rocks and concrete.

ACKNOWLEDGEMENTS

Special thanks to Professor Brown (developer of the Hoek–Brown criterion) for sharing the biaxial compression test data of rocks (Figure 8A and reference herein[7]) and his valuable suggestions in development of the new 3D Hoek–Brown criterion. The first author also acknowledges the financial support from the Natural Science Foundation of Shaanxi Province (grant 211421180224) and the Fundamental Research Funds for the Central Universities (grant 300102218201).

LIST OF SYMBOLS

$\sigma_1,\sigma_2,\sigma_3$	principal stresses at failure
σ,S	stress tensor and deviatoric stress tensor
I_1	first invariant of stress tensor and the mean stress
J_2,J_3	second and third invariants of deviatoric stress tensor
$\sigma'_1,\sigma'_2,\sigma'_3$	effective principal stresses at failure
ξ,ρ,θ	Haigh–Westergaard coordinates
m_b,s,a	empirical constants of the generalized Hoek–Brown criterion
σ_{ci},m_i	uniaxial compression strength and material constant of intact rock
GSI, D	geological strength index and the disturbance of rock masses
$B(\theta),C(\theta)$	coefficient of the HB criterion in terms of the stress invariants
$A(\theta)$	coefficient of the general expression of the 3D HB criteria
$R_3(\theta)$	elliptic Lode dependence function
$\lambda(\theta, k)$	inverse of the elliptic Lode dependence function
k	additional parameter in the new 3D HB criterion
ρ_c,ρ_t	compression and extension meridian radii of the failure criterion
e	meridian radius ratio of the extension and compression meridian radius
$\sigma_{1i}^{test},\sigma_{1i}^{calc}$	ith tested and calculated strength
n	number of test series for a specific rock or concrete
$RMSE$	root-mean-square error
DC	coefficient of determination
TXC, TXE, PXC	triaxial compression, triaxial extension, and polyaxial compression
f_{cc}, f_t	equibiaxial compression strength and uniaxial tension strength
$\sigma'_{2,intersect}$	value of σ'_2 where the solid curve insects with the dashed curve

ORCID

Hua Jiang https://orcid.org/0000-0002-2625-4303
Yang Yang https://orcid.org/0000-0003-1686-739X

REFERENCES

1. Hoek E, Brown ET. Empirical strength criterion for rock masses. *J Geotech Engng ASCE*. 1980;106(GT9):1013-1035.
2. Hoek E, Carranza-Torres C, Corkum B. Hoek–Brown failure criterion—2002 edition. In: Hammah R et al., eds. *Proc. 5th North American Rock Mech. Symp and 17th Tunneling. Assoc. of Canada Conf.: NARMS-TAC*. Toronto: Mining Innovation and Tech; 2002:267-273.
3. Hoek E, Brown ET. The Hoek–Brown failure criterion and GSI–2018 edition. *J Rock Mech Geotech Eng*. 2019;11(3):445-463.
4. Mogi K. Effect of the intermediate principal stress on rock failure. *J Geophys Res*. 1967;72(20):5117-5131.
5. Mogi K. Fracture and flow of rocks under high triaxial compression. *J Geophys Res*. 1971;76(5):1255-1269.
6. Mogi K. *Experimental rock mechanics*. London: Taylor & Francis; 2007.
7. Brown ET. Fracture of rock under uniform biaxial compression. In: Proc., 3rd Congress of International Society for Rock Mechanics. Denver, CO, USA, 111–117. 1974.
8. Michelis P. A true triaxial cell for low and high pressure experiments. *Int. J. Rock Mech. Min. Sci. & Geomech. Abstr*. 1985;22(3):183-188.
9. Michelis P. Polyxial yielding of granular rock. *J Eng Mech ASCE*. 1985;111(8):1049-1066.
10. Takahashi M, Koide H. Effect of the intermediate principal stress on strength and deformation behavior of sedimentary rocks at the depth shallower than 2000 m. In: Maury V, Fourmaintraux D, eds. *Rock at Great Depth*. Vol.1 Rotterdam: Balkema; 1989:19-26.
11. Haimson B, Chang C. A new true triaxial cell for testing mechanical properties of rock, and its use to determine rock strength and deformability of Westerly granite. *Int J Rock Mech Min Sci*. 2000;37(1-2):285-296.
12. Chang C, Haimson BC. True triaxial strength and deformability of the German Continental deep drilling program (KTB) deep hole amphibolite. *J Geophys Res*. 2000;105(B8):18999-19013.
13. Lee H, Haimson B. True triaxial strength, deformability, and brittle failure of granodiorite from the San Andreas Fault Observatory at Depth. *Int J Rock Mech Min Sci*. 2011;48(7):1199-1207.
14. Ma X, Haimson B. Failure characteristics of two porous sandstones subjected to true triaxial stresses. *J Geophys Res Solid Earth*. 2016;121:1-22.
15. Alex V, Ahmad G. Failure characteristics of three shales under true-triaxial compression. *Int J Rock Mech min Sci*. 2017;100:151-159.
16. Feng X, Kong R, Zhang X, Yang C. Experimental study of failure differences in hard rock under true triaxial compression. *Rock Mech Rock Eng*. 2019;52(7):2109-2122.
17. Du K, Yang C, Su R, Tao M, Wang S. Failure properties of cubic granite, marble, and sandstone specimens under true triaxial stress. *Int J Rock Mech min Sci*. 2020;130:1–15, 104309.
18. Haimson B. True triaxial stresses and the brittle fracture of rock. *Pure Appl Geophys*. 2006;163(5-6):1101-1130.
19. Feng X, Haimson B, Li X, et al. ISRM suggested method: determining deformation and failure characteristics of rocks subjected to true Triaxial compression. *Rock Mech Rock Eng*. 2019;52(6):2011-2020.
20. Priest SD. ISRM suggested method: Three-dimensional failure criteria based on the Hoek–Brown criterion. *Rock Mech Rock Eng*. 2012;45(6):989-993.
21. Jiang H, Wang XW, Xie YL. New strength criteria for rocks under polyaxial compression. *Canadian Geotechnical Journal*. 2011;48(8):1233-1245.
22. Lee YK, Pietruszczak S, Choi BH. Failure criteria for rocks based on smooth approximations to Mohr–Coulomb and Hoek–Brown failure functions. *Int J Rock Mech min Sci*. 2012;56:146-160.
23. Zhang Q, Zhu H, Zhang L. Modification of a generalized three-dimensional Hoek–Brown strength criterion. *Int J Rock Mech min Sci*. 2013;59:80-86.
24. Jiang H, Zhao JD. A simple three-dimensional failure criterion for rocks based on the Hoek–Brown criterion. *Rock Mech Rock Eng*. 2015;48(5):1807-1819.
25. Jiang H. Three-dimensional failure criteria for rocks based on the Hoek–Brown criterion and a general lode dependence. *Int J Geomech*. 2017;17(8):04017023-1–04017023-12.
26. Pan XD, Hudson JA. A simplified three dimensional Hoek–Brown yield criterion. *Rock Mech Power Plants*. 1998;95-103.
27. Priest SD. Determination of shear strength and three-dimensional yield strength for the Hoek–Brown criterion. *Rock Mech Rock Eng*. 2005;38(6):299-327.
28. Melkoumian N, Priest SD, Hunt SP. Further development of the three-dimensional Hoek–Brown yield criterion. *Rock Mech Rock Eng*. 2008;42(6):835-847.
29. Zhang L, Zhu H. Three-dimensional Hoek–Brown strength criterion for rocks. *J Geotech Geoenviron Eng*. 2007;133(9):1128-1135.
30. Zhang L. A generalized three-dimensional Hoek–Brown strength criterion. *Rock Mech Rock Eng*. 2008;41(4):893-915.
31. Priest SD. Comparisons between selected three-dimensional yield criteria applied to rock. *Rock Mech Rock Eng*. 2009;43:379-389.
32. Jiang H, Xie YL. A note on the Mohr–Coulomb and Drucker–Prager strength criteria. *Mechanics Research Communications*. 2011;38(4):309-314.
33. Jiang H, Xie YL. A new three-dimensional Hoek–Brown strength criterion. *Acta Mech Sin*. 2012;28(2):393-406.
34. Hsieh SS, Ting EC, Chen WF. An elastic fracture model for concrete. In Proceedings of the 3rd Engineering Mechanics Division Specialty Conference, Austin, Tex., 17–19. September 1979. American Society of Civil Engineers (ASCE), Reston, Va. pp 437–440.

35. Murrell SAF. A criterion for brittle fracture of rocks and concrete under triaxial stress, and the effect of pore pressure on the criterion. In: Fairhurst C, ed. *Proceedings of the 5th Symposium on Rock Mechanics*. Minneapolis: University of Minnesota; 1963:563-577.
36. Handin J, Heard HC, Magouirk JN. Effect of the intermediate principal stress on the failure of limestone, dolomite, and glass at different temperature and strain rate. *J Geophys Res*. 1967;72(2):611-640.
37. Phueakphum D, Fuenkajorn K, Walsri C. Effects of intermediate principal stress on tensile strength of rocks. *Int J Fract*. 2013;181(2): 163-175.
38. Hackston A, Rutter EH. The Mohr–Coulomb criterion for intact rock strength and friction-a re-evaluation and consideration of failure under polyaxial stresses. *Solid Earth*. 2016;7(2):493-508.
39. Mills LL, Zimmerman RM. Compressive strength of plain concrete under multiaxial loading conditions. *ACI J Proc*. 1970;802-807.
40. Kupfer H, Hilsdorf HK, Rusch H. Behavior of concrete under biaxial stresses. *ACI J*. 1969;66(8):545-666.
41. Launay P, Gachon H. Strain and ultimate strength of concrete under triaxial stresses. *ACI Spec Pub*. 1972;1:269-282.
42. Chen WF, Saleeb AF. *Constitutive Equations for Engineering Materials: Elasticity and Modeling*. 1 Amsterdam, Netherlands: Elsevier; 1994.
43. Lee YK, Bobet A. Instantaneous friction angle and cohesion of 2-D and 3-D Hoek–Brown rock failure criteria in terms of stress invariants. *Rock Mech Rock Eng*. 2014;47(2):371-385.
44. Willam KJ, Warnke EP. Constitutive model for the triaxial behavior of concrete. Presented at the seminar on concrete structures subjected to triaxial stress. Istituto Sperimentale Modellie Strutture (ISMES), Bergamo,1–30. 1975.
45. Colmenares LB, Zoback MD. A statistical evaluation of intact rock failure criterial constrained by polyaxial test data for five different rocks. *Int J Rock Mech min Sci Sci*. 2002;39(6):695-729.
46. RocData. Rocdata 4.0.2012. http://www.rocscience.com/products/4/RocData
47. Oda M, Nakayama H. Yield function for soil with anisotropic fabric. *J EngMech ASCE*. 1989;115(1):89-104.
48. Pietruszczak S, Mroz Z. Formulation of anisotropic failure criteria incorporating a microstructure tensor. *Comput Geotech*. 2000;26(2): 105-112.
49. Lade PV. Modeling failure in cross-anisotropic frictional materials. *Int J Solid Struct*. 2007;44(16):5146-5162.
50. Gao Z, Zhao J, Yao Y. A generalized anisotropic failure criterion for geomaterials. *Int J Solid Struct*. 2010;47(22–23):3166-3185.

How to cite this article: Jiang H, Yang Y. A three-dimensional Hoek–Brown failure criterion based on an elliptical Lode dependence. *Int J Numer Anal Methods Geomech*. 2020;44:2395–2411. https://doi.org/10.1002/nag.3125